STEM CELLS TRANSLATIONAL MEDICINE®

TISSUE ENGINEERING AND REGENERATIVE MEDICINE

Allogeneic Mesenchymal Stem Cell Therapy Promotes Osteoblastogenesis and Prevents Glucocorticoid-Induced Osteoporosis

BINGDONG SUI,[a,b,c,d,*] CHENGHU HU,[a,b,*] XINYI ZHANG,[a,b] PAN ZHAO,[a,b] TAO HE,[a,b] CUIHONG ZHOU,[a,b] XINYU QIU,[a,b] NAN CHEN,[a,b] XINYI ZHAO,[c,d] YAN JIN[a,b]

Key Words. Glucocorticoid-induced osteoporosis • Mesenchymal stem cell therapy • Cell homing • Bone remodeling • Osteoblastogenesis

[a]State Key Laboratory of Military Stomatology, Center for Tissue Engineering, [b]Research and Development Center for Tissue Engineering, [c]State Key Laboratory of Military Stomatology, Department of Dental Materials, and [d]Department of Dental Materials, School of Stomatology, Fourth Military Medical University, Xi'an, Shaanxi, People's Republic of China

[*]Contributed equally.

Correspondence: Yan Jin, M.D., Ph.D., Research and Development Center for Tissue Engineering, Fourth Military Medical University, No. 145 West Changle Road, Xi'an, Shaanxi 710032, People's Republic of China. Telephone: 86-029-84776472; E-Mail: yanjin@fmmu.edu.cn; or Xinyi Zhao, M.D., Ph.D., Department of Dental Materials, School of Stomatology, Fourth Military Medical University, No. 145 West Changle Road, Xi'an, Shaanxi 710032, People's Republic of China. Telephone: 86-029-84776177; E-Mail: zhaoxinyi@fmmu.edu.cn

Received November 30, 2015; accepted for publication April 7, 2016; published Online First on June 30, 2016.

1066-5099/2016/$20.00/0

http://dx.doi.org/10.5966/sctm.2015-0347

ABSTRACT

Gene-modified mesenchymal stem cell (MSC)-like cells with enhanced bone marrow homing and osteogenesis have been used in treating glucocorticoid-induced murine osteoporosis (GIOP). Recent preclinical studies have further demonstrated the immunomodulatory and anticatabolic potential of allogeneic MSCs in treating osteoporosis under inflammatory and autoimmune conditions. In this study, we investigated whether systemic infusion of allogeneic MSCs without genetic manipulation could prevent GIOP, whether anabolic and anticatabolic effects existed, and whether homing or immunomodulation underlay the putative therapeutic effects. Allogeneic bone marrow-derived MSCs (BMMSCs) were isolated, identified, and systemically infused into mice treated with excessive dexamethasone. We revealed that allogeneic MSC transplantation prevented the reduction of bone mass and strength in GIOP. Bone histomorphometric analyses of bone remodeling demonstrated the maintenance of bone formation and osteoblast survival after MSC therapy. Using green fluorescent protein (GFP)-labeled BMMSCs, we showed that donor BMMSCs^{GFP} homed and inhabited recipient bone marrow for at least 4 weeks and prevented recipient bone marrow cell apoptosis, as shown by terminal deoxynucleotidyl transferase-mediated dUTP nick-end labeling. Furthermore, donor BMMSCs^{GFP} committed to Osterix (Osx)$^{+}$ osteoblast progenitors and induced recipient osteoblastogenesis, as exhibited by GFP-Osx double-labeling immunofluorescence analysis. No anticatabolic effects or systemic immunomodulatory effects of infused BMMSCs were detected. These findings demonstrated that allogeneic MSC therapy prevented GIOP by inhabiting and functioning in recipient bone marrow, which promoted osteoblastogenesis, which in turn maintained bone formation. Our findings provide important information regarding cell-based anabolic therapy for GIOP and uncover MSC behaviors following the homing event. STEM CELLS TRANSLATIONAL MEDICINE *2016;5:1238–1246*

SIGNIFICANCE

This study revealed the therapeutic potential of systemically infused, genetically unmodified allogeneic MSCs in glucocorticoid-induced osteoporosis. The donor MSCs inhabited recipient bone marrow and promoted osteoblastogenesis. The therapeutic effects were based on maintenance of bone formation. These results provide important information regarding cell-based anabolic therapy for glucocorticoid-induced osteoporosis and uncover previously unrecognized mesenchymal stem cell behaviors following a homing event. The current study also indicates that minimizing the time of cell culture confers an advantage for increasing transplanted mesenchymal stem cells to the targeted organ to promote therapeutic effects.

INTRODUCTION

Glucocorticoid-induced osteoporosis (GIOP) is the most prevalent form of secondary osteoporosis, the key feature of which is the rapid reduction of bone formation [1–4]. Mesenchymal stem cells (MSCs, also known as mesenchymal stromal cells), recognized as osteoblastic precursors, have shown therapeutic prospects in the prevention and management of osteoporotic bone loss in preclinical studies [5–10]. In murine GIOP, Lien et al. restored bone mass and strength by systemic infusion of C3H10T1/2 MSC-like cells [5], which were transduced to ectopically express CXC chemokine receptor 4 (CXCR4), the receptor for stroma-derived factor 1 (SDF-1) [11], to facilitate bone marrow homing and retention efficacy, and core binding factor α1 (Cbfα-1), an osteoblast master transcription factor [12], to promote osteogenic differentiation postengraftment.

Recently, preclinical studies have further revealed that based on immunomodulation, allogeneic MSCs without genetic manipulation exhibited profound potential to inhibit bone resorption and ameliorate osteoporosis under inflammatory and autoimmune conditions [8–10]. Whether allogeneic MSCs hold therapeutic effects in GIOP is unknown.

According to reported data, transplanted MSCs rescue bone loss through either systemic immunomodulatory and anticatabolic effects [8–10] or local anabolic effects exerted via direct intrabone marrow injection or cell homing postinfusion [5–7]. Given that glucocorticoid therapy is widely used in autoimmune diseases to control inflammation [1], immunomodulation might not contribute to the putative effects of allogeneic MSCs in treating GIOP. Alternatively, Lien and others demonstrated that intravenously (i.v.) transplanted MSCs could migrate and nonspecifically distribute in various organs including lung and liver, or preferentially home, with limited efficiency, to bone marrow [5, 13, 14]. Without transduction to enforce homing, it remains to be elucidated whether systemically infused allogeneic MSCs could inhabit and function in recipient bone marrow to maintain therapeutic effects in GIOP.

In this study, we aimed to (a) examine whether allogeneic MSC therapy via systemic infusion can prevent the development of GIOP, (b) investigate whether anabolic and anticatabolic effects exist, and (c) elucidate whether homing or immunomodulation underlie the putative therapeutic effects. We hypothesized that allogeneic MSC therapy could prevent the reduction of bone mass and strength in GIOP through maintaining bone formation by inhabiting and functioning in recipient bone marrow.

Materials and Methods

Animals and Experimental Design

The Guidelines of Intramural Animal Use and Care Committee of the Fourth Military Medical University were followed. Female wild-type (WT) C57BL/6 mice (age, 12 weeks; weight, 20–22 g) (Laboratory Animal Center, the Fourth Military Medical University, China) and female green fluorescent protein $(GFP)^{+/+}$ transgenic mice (age, 12 weeks; weight, 20–22 g) (C57BL/6 background, the Fourth Military Medical University, China) were used. The mice were allowed to eat and drink ad libitum before being sacrificed.

Experiment 1: Effects of Systemically Infused MSCs in the Prevention of GIOP

WT mice were randomized by weight into four groups ($n = 4$ each) according to treatment. In the GIOP group, mice received 20 mg/kg/day intraperitoneal (i.p.) dexamethasone (DEX) (Sigma-Aldrich, St. Louis, MO, http://www.sigmaaldrich.com) for 35 consecutive days, as previously reported [5]. DEX was dissolved in phosphate-buffered saline (PBS) (Thermo Fisher Scientific Life Sciences, Waltham, MA, http://www.thermofisher.com) in a final concentration of 2 mg/ml, and one DEX injection was given daily at 10 μl/g. In the control group, mice received 10 μl/g PBS for 5 weeks i.p. Necessary precautions were taken to prevent the injected fluid from being accidentally placed in intestine. In the GIOP+BMMSC group, 1×10^6 donor bone marrow MSCs (BMMSCs) derived from WT mice were suspended in 200 μl PBS and intravenously (i.v.) infused into each recipient GIOP mouse on day 7 of GIOP injection [5, 9]. In the GIOP+PBS group, equivalent PBS was infused. Nothing (vehicle) was infused into mice of the control group and the GIOP group. Mice were sacrificed on day 35 of GIOP injection. Femora were sampled for the micro-computed tomography (micro-CT) analysis for bone mass evaluation, and tibiae were collected for three-point bending test for bone quality determination.

Experiment 2: Effects of MSC Therapy on Bone Remodeling in GIOP

WT mice were randomized by weight into three groups ($n = 4$ each): control, GIOP+PBS, and GIOP+BMMSC. Control and GIOP modeling, as well as the systemic infusion of PBS and BMMSCs, was according to methods stated above. Mice were sacrificed on day 35 of GIOP injection. Sixteen and 2 days before sacrifice, mice received double i.p. injection of 20 mg/kg calcein (Sigma-Aldrich) [15]. Just before sacrifice, whole peripheral blood was sampled for enzyme-linked immunosorbent assay (ELISA). At sacrifice, femora were sampled for calcein labeling and immunofluorescent examination, and tibiae were collected for tartrate resistant acid phosphatase (TRAP) and toluidine blue staining.

Experiment 3: Fates of Infused MSCs in GIOP Mice

$GFP^{+/+}$ mice were used as BMMSC donors. WT recipient mice were randomized by weight into three groups ($n = 8$ each): control, GIOP+PBS, and GIOP+BMMSC. Control and GIOP modeling, as well as the systemic infusion of PBS and $BMMSCs^{GFP}$, was according to methods stated above. At 4, 24, and 72 hours after $BMMSC^{GFP}$ infusion ($n = 4$ each), mice of the GIOP+BMMSC group were randomly chosen and 50 μl peripheral blood was sampled from the tail for flow cytometric analysis to determine of the survival of GFP^+ cells in the peripheral blood. Mice of the GIOP+PBS group also underwent blood sampling 24 hours after PBS infusion. Mice were kept alive after blood sampling. At 24 hours ($n = 4$) and 4 weeks ($n = 4$) after PBS or $BMMSC^{GFP}$ infusion, mice of all three groups were randomly chosen and sacrificed to collect femora for immunofluorescent tests and whole peripheral blood for ELISA.

BMMSC or $BMMSC^{GFP}$ Culture, Identification, and Systemic Infusion

For Experiments 1 and 2, BMMSCs were derived from C57BL/6 mice. For Experiment 3, $BMMSCs^{GFP}$ were sourced from $GFP^{+/+}$ transgenic mice. Isolation and culture of murine BMMSCs and $BMMSCs^{GFP}$ were as previously described [16, 17]. Briefly, murine bone marrow cells were seeded, incubated overnight, and rinsed with PBS to remove nonadherent cells. Adherent cells were cultured with α-minimum essential medium supplemented with 20% fetal bovine serum (FBS), 2 mM L-glutamine, 100 U/ml penicillin, and 100 g/ml streptomycin (all from Thermo Fisher Scientific Life Sciences) at 37°C in a humidified atmosphere of 5% CO_2. BMMSCs were identified by colony formation, morphology, osteogenic and adipogenic differentiation, and surface marker analysis, as stated below. Primary BMMSC or $BMMSC^{GFP}$ colonies were applied for infusion after digestion with 0.25% trypsin (MP Biomedicals, Santa Ana, CA, http://www.mpbio.com) to yield appropriate numbers ($2–3 \times 10^6$ BMMSCs or $BMMSCs^{GFP}$ could be harvested from one mouse).

For systemic infusion, BMMSCs were suspended in PBS at 5×10^6/ml and put on ice. BMMSCs or $BMMSCs^{GFP}$ (1×10^6 in 200 μl or equivalent PBS) were administered via caudal vein into each recipient mouse on day 7 of DEX treatment, which was finished within 30 minutes after digestion [8, 9]. For colony formation analysis, primary BMMSCs at confluence were digested and plated in 5-cm culture dishes at a density of 1×10^4 cells/dish.

After 14 days of culture, the colonies were fixed with 4% paraformaldehyde for 30 minutes and stained with crystal violet (Sigma-Aldrich) for 5 minutes [18]. For cell morphologic evaluation, primary BMMSCs at confluence were digested and plated in six-well plates at a density of 5×10^5 cells/well. After 1 day of culture, cell morphology was evaluated and photographs were taken.

For osteogenic differentiation, seeded BMMSCs were further induced in osteogenesis-inducing media containing 100 μg/ml ascorbic acid (MP Biomedicals), 2 mM β-glycerophosphate (Sigma-Aldrich), and 10 nM DEX. After induction for 14 days, alizarin red (Sigma-Aldrich) staining was performed to determine mineralization [16]. For adipogenic differentiation, seeded BMMSCs were further induced in adipogenesis-inducing media containing 0.5 mM isobutylmethylxanthine (MP Biomedicals), 0.5 mM DEX, and 60 mM indomethacin (MP Biomedicals). After induction for 14 days, oil red O (Sigma-Aldrich) staining was performed to determine lipid droplet formation. Photographs were all taken using an inverted optical microscope (CKX41; Olympus, Tokyo, Japan, http://www.olympusamerica.com) [16].

For flow cytometric analysis of surface makers, primary BMMSC colonies were digested and suspended in PBS supplemented with 3% FBS at 1×10^6 cells/ml. Added to this were 2×10^5 cells/tube with 1 μl fluorescein isothiocyanate (FITC)-conjugated anti-mouse CD11b antibody, 1 μl phycoerythrin (PE)-conjugated anti-mouse CD29 antibody, 1 μl PE-conjugated anti-mouse CD34 antibody, 1 μl PE-conjugated anti-mouse CD45 antibody, 1 μl PE-conjugated anti-mouse vascular cell adhesion molecule 1 (VCAM1, also known as CD106) antibody, and 1 μl FITC-conjugated anti-mouse stem cell antigen 1 (Sca-1) antibody (all from Abcam, Cambridge, MA, http://www.abcam.com). Nonimmune immunoglobulin of the same isotype was used as the negative control. BMMSCs were incubated at 4°C for 30 minutes in the dark and washed twice with PBS supplemented with 3% FBS. The percentage of positively stained cells was determined with a flow cytometer (FACSAria; BD, Franklin Lakes, NJ, http://www.bd.com) equipped with FACSDiva version 6.1.3 software [19].

Micro-CT Analysis for Bone Mass Evaluation

For trabecular and cortical bone mass evaluation, a desktop micro-CT system (eXplore Locus SP, GE Healthcare, Little Chalfont, U.K., http://www3.gehealthcare.com) was used, as previously documented [20]. In Experiment 1, at sacrifice, the left femora were removed, fixed overnight in 4% paraformaldehyde, and prepared into 1-mm blocks with the distal femoral metaphysis included. The specimens were scanned at a resolution of 8 μm, a voltage of 80 kV, and a current of 80 μA. Trabecular bone data were obtained at a region of interest (ROI) in the distal metaphysis, 0.3–0.8 mm away from the epiphysis. Cortical ROI was defined in the midshaft, 3.3–3.8 mm away from the epiphysis. Data were analyzed with the Micview V2.1.2 software, and quantification was performed using parameters of bone volume per tissue volume, bone mineral density, trabecular bone thickness, trabecular bone number, trabecular separation, cortical bone thickness, total cross-sectional area inside the periosteal envelope, cortical bone area, and cortical bone area fraction [9, 21].

Three-Point Bending Test for Bone Quality Determination

Tibiae were used for mechanical testing for bone quality determination in Experiment 1. At sacrifice, the left tibiae were isolated, and the length was measured using a caliper to determine midpoint. The tibiae were then placed in a universal testing machine (AGS-10KN; Shimadzu, Kyoto, Japan, http://www.shimadzu.com) with two lower supports at a distance of 15 mm. The load was applied to the midpoint at a displacement rate of 0.05 mm/s until failure. The displacement, load, and load-deformation curve were recorded. Ultimate force was defined as the maximal load. Young's modulus was calculated according to Turner and Burr [22].

Bone Histomorphometric Analyses for Bone Remodeling Evaluation

For bone formation examination, double calcein labeling was performed according to previous studies, with minor modifications [15, 20] (supplemental online Fig. 3A). In Experiment 2, at 16 and 2 days before sacrifice, mice received double injection i.p. of 20 mg/kg calcein. Calcein was dissolved at a concentration of 2 mg/ml in PBS supplemented with 1 mg/ml $NaHCO_3$ (Sigma-Aldrich) and was injected at 10 μl/g each time away from light. Necessary precautions were taken to ensure that the injected fluid was never accidentally placed in intestine, and that successful administration of double calcein labeling was accomplished in all mice. At sacrifice, left femora were isolated, fixed in 80% ethanol, and embedded in methyl methacrylate. The specimens were sagittally sectioned into 30-μm sections using a hard tissue slicing machine (SP1600; Leica, Munich, Germany, http://www.leica.com) away from light. Both double-labeled and single-labeled cortical endosteum surfaces were evaluated by a fluorescence microscope (STP6000; Leica) with an excitation wavelength of 488 nm. Quantification was performed based on at least five photographs using the parameters of mineral apposition rate (MAR) and mineralized surface per bone surface (MS/BS). Bone formation rate (BFR) was calculated as MAR $\times$ MS/BS, according to previous studies [15].

For osteoblast and osteoclast/bone resorption examination, toluidine blue and TRAP staining was performed, as stated previously [23]. In Experiment 2, at sacrifice, tibiae were isolated, fixed with 4% paraformaldehyde, decalcified with 10% ethylene diamine tetraacetic acid (EDTA) (pH 7.2–7.4), and embedded in paraffin. Sagittal serial sections (5 μm) of proximal metaphyses were prepared (RM2125; Leica). The sections were stained by 1% toluidine blue (Sigma-Aldrich) dissolved in PBS for 30 minutes or by TRAP using a commercial kit according to the manufacturer's instructions (387-1A; Sigma-Aldrich). Osteoblast quantification was performed using the parameters of number of osteoblasts per bone surface and osteoblast surface per bone surface [15]. Similarly, osteoclast/bone resorption quantification was determined using the parameters of number of osteoclasts per bone surface and osteoclast surface per bone surface [15]. Quantification was performed using ImageJ 1.47 software from at least five consecutive microscopic fields.

ELISA for the Detection of Serological Markers

In Experiments 2 and 3, at 24 hours and 4 weeks after PBS or BMMSC infusion, before necropsy, 500-μl samples of whole peripheral blood were collected from the retro-orbital venous plexus. Sera were isolated by centrifuging at 3,000 rpm for 10 minutes followed by 12,000 rpm for 10 minutes at 4°C [9]. Markers for bone formation (procollagen 1 N-terminal peptide [P1NP]), bone resorption (cross-linked C-telopeptide of type 1 collagen [CTX-1]), and inflammation (tumor necrosis factor [TNF]-α and interferon [IFN]-γ) were detected using murine ELISA kits according to the

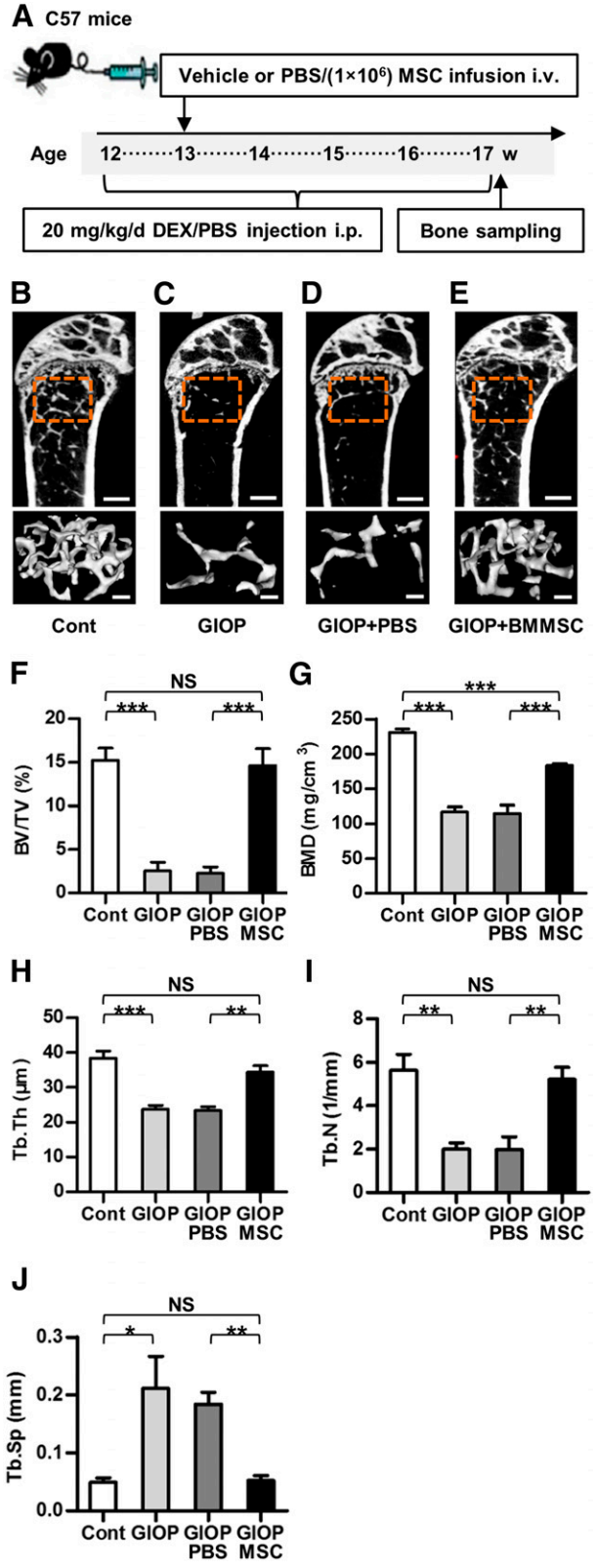

Figure 1. Study design of Experiment 1 and trabecular bone mass. **(A):** Study design of the Experiment 1 for bone mass evaluation. Femora and the tibiae were sampled at sacrifice. **(B–E):** Representative micro-CT images illustrating trabecular bone mass of the distal metaphyses of femora. ROI was defined 0.3–0.8 mm away from epiphyses. Scale bars: 500 μm (top) and 100 μm (bottom). **(F–J):** Corresponding parameters showing prevention of GIOP by MSC therapy. Data represent mean ± SEM; $n = 4$ per group. **, $p < .01$; ***, $p < .001$. Abbreviations: BMD, bone mineral density; BMMSC, bone marrow-derived mesenchymal stem cell; BV/TV, bone volume per tissue volume; Cont, control; DEX, dexamethasone; GIOP, glucocorticoid-induced osteoporosis; i.p., intraperitoneally; i.v., intravenously; micro-CT, micro-computed tomography; MSC, mesenchymal stem cell; NS, not significant; PBS, phosphate-buffered saline; ROI, region of interest; Tb.N, trabecular bone number; Tb.Th, trabecular bone thickness; Tb.Sp, trabecular separation; w, weeks.

manufacturer's instructions (R&D Systems, Minneapolis, MN, http://www.rndsystems.com).

Immunofluorescent Staining and Terminal Deoxynucleotidyl Transferase-Mediated dUTP Nick-End Labeling

In Experiments 2 and 3, at sacrifice, femora were isolated, fixed in 4% paraformaldehyde, cryoprotected with 30% sucrose, decalcified with 10% EDTA (pH 7.2–7.4), and embedded in optimal cutting temperature compound. The specimens were snap-frozen and sectioned into 15-μm sagittal sections (CM1950; Leica). All of the below antibodies were from Cell Signaling Technology (Danvers, MA, http://www.cellsignal.com). Nonimmune immunoglobulin of the same isotype was used as the negative control. Sections were observed under a fluorescence microscope (DP70; Olympus). The images were further analyzed using ImageJ 1.47 software from at least five consecutive microscopic fields.

In the Experiment 2, right femora were evaluated for in situ detection of osteoblast progenitors in bone marrow. Osteoblast progenitors were identified with Osterix (Osx) [24]. Sections were blocked with 5% bovine serum albumin (Sigma-Aldrich) dissolved in PBS for 1 hour at room temperature. Sections were then stained with a goat anti-Osx primary antibody for 2 hours at room temperature at a concentration of 1:100, followed by donkey anti-goat-FITC secondary antibody for 30 minutes at room temperature at a concentration of 1:200. Sections were counterstained with Hoechst (Sigma-Aldrich) for 3 minutes at room temperature.

In Experiment 3, left femora were evaluated for in situ detection of donor BMMSCs^{GFP} in recipient bone marrow [17]. Sections were blocked as stated. Sections were then stained with rabbit anti-GFP primary antibody for 2 hours at room temperature at a concentration of 1:100, followed by goat anti-rabbit-FITC secondary antibody for 30 minutes at room temperature at a concentration of 1:200, and counterstained with Hoechst as stated.

For in situ detection of apoptosis of both donor BMMSCs^{GFP} and recipient bone marrow cells, terminal deoxynucleotidyl transferase-mediated dUTP nick-end labeling (TUNEL) and GFP-immunofluorescence double-labeling assays were performed, as previously reported [25]. Briefly, sections from the right femora underwent TUNEL assay using DeadEnd Colorimetric TUNEL System according to the manufacturer's instructions (Promega, Madison, WI, http://www.promega.com). Sections were blocked, stained for anti-GFP primary antibody and the secondary antibody, and counterstained with Hoechst, as stated above.

For in situ detection of osteogenic differentiation of both donor BMMSC^{GFP} and recipient BMMSCs, an Osx- and GFP-immunofluorescence double-labeling assay was performed. Sections were blocked as stated. Sections were then costained with goat anti-Osx primary antibody and rabbit anti-GFP primary antibody for 2 hours at room temperature at a concentration of 1:100,

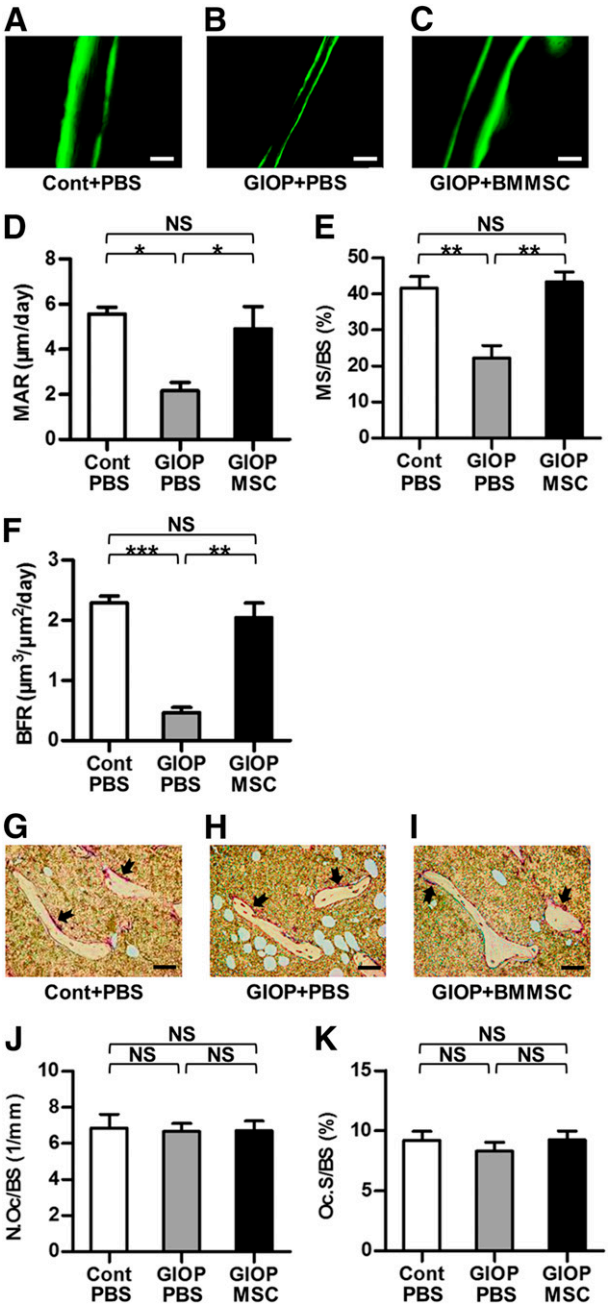

Figure 2. Bone formation and bone resorption parameters. **(A–C):** Representative calcein-labeling images exhibiting bone formation rates. Mice received double injection of 20 mg/kg calcein at 16 and 2 d before sacrifice. Scale bars: 100 μm. **(D–F):** Corresponding parameters showing maintenance of bone formation by MSC therapy. **(G–I):** Representative TRAP-staining images exhibiting bone resorption rates. Red-stained areas with black arrows indicate osteoclasts. The unstained area in the bone marrow represents empty spaces occupied by adipocytes. Scale bars: 50 μm. **(J, K):** Corresponding parameters showing paralleled bone resorption. Data represent mean ± SEM; $n = 4$ per group. *, $p < .05$; **, $p < .01$; and ***, $p < .001$. Abbreviations: BFR, bone formation rate; BMMSC, bone marrow-derived mesenchymal stem cell; Cont, control; GIOP, glucocorticoid-induced osteoporosis; MAR, mineral apposition rate; MS/BS, mineralized surface per bone surface; MSC, mesenchymal stem cell; N.Oc/BS, number of osteoclasts per bone surface; NS, not significant; Oc.S/BS, osteoclast surface over bone surface; PBS, phosphate-buffered saline; TRAP, tartrate resistant acid phosphatase.

followed by donkey anti-goat-cyanine 3 secondary antibody together with a goat anti-rabbit-FITC secondary antibody for 30 minutes at room temperature at a concentration of 1:200, and counterstained with Hoechst as stated.

Flow Cytometric Analysis for Detection of Donor BMMSCs^{GFP} in Recipient Peripheral Blood

In Experiment 3, 50-μl blood samples were collected by cutting off the tips of the tails at indicated times. Samples were treated with ACK lysis buffer (Lonza, Basel, Switzerland, http://www.lonza.com) to remove red blood cells and washed with PBS. Percentages of GFP$^+$ cells in peripheral blood mononuclear cells (PBMNCs) were determined with a flow cytometer (Cytomics FC 500; Beckman-Coulter, Danvers, MA, https://www.beckmancoulter.com) equipped with CXP 2.1 software.

Statistical Analysis

All results are presented as mean ± SEM. The data were analyzed using one-way analysis of variance followed by post hoc tests of Newman-Keuls multiple comparison in GraphPad Prism software. Values of $p < .05$ were considered statistically significant.

Results

Systemic Infusion of Allogeneic BMMSCs Maintained Bone Mass and Strength in Glucocorticoid-Treated Mice

Murine BMMSCs used in the present study were demonstrated to have the potential to form colonies and differentiate into multilineage osteoblasts and adipocytes (supplemental online Fig. 1A–1D), as reported in our previous research [16, 26]. Analyzed by flow cytometry, these BMMSCs uniformly expressed surface makers considered to represent mesenchymal stem cells, including CD29, VCAM1, and Sca-1, but were negative for hematopoietic markers CD11b, CD34, and CD45 (supplemental online Fig. 1E) [19, 26].

To explore the therapeutic potential of allogeneic MSCs in GIOP, we infused BMMSCs systemically into glucocorticoid-treated mice according to the study design of Experiment 1 (Fig. 1A). Micro-CT analysis demonstrated that BMMSC infusion maintained trabecular bone mass in glucocorticoid-treated mice (Fig. 1B–1E) with corresponding improvements in trabecular bone volume (Fig. 1F), mineral density (Fig. 1G), thickness (Fig. 1H), number (Fig. 1I), and separation (Fig. 1J). Additional analysis showed partial prevention against cortical bone loss by MSC therapy (supplemental online Fig. 2A–2D), as indicated by the improvements of cortical bone thickness (supplemental online Fig. 2E) and cortical area fraction (supplemental online Fig. 2F–2H). Mechanical tests further demonstrated partial maintenance of bone strength by systemic infusion of BMMSCs, as shown in supplemental online Fig. 2I and 2J.

Allogeneic BMMSC Infusion Prevented GIOP Through Maintenance of Bone Formation

To explore the underlying mechanisms of the therapeutic effects of BMMSC infusion in GIOP, we analyzed bone-remodeling parameters in Experiment 2 (supplemental online Fig. 3A). Calcein labeling showed rescue of the impaired bone formation by BMMSC infusion (Fig. 2A–2C) with almost complete maintenance of MAR (Fig. 2D), MS/BS (Fig. 2E), and BFR (Fig. 2F). However, no significant changes were found in bone resorption, as shown by TRAP staining on osteoclasts (Fig. 2G–2K). Detection of serological

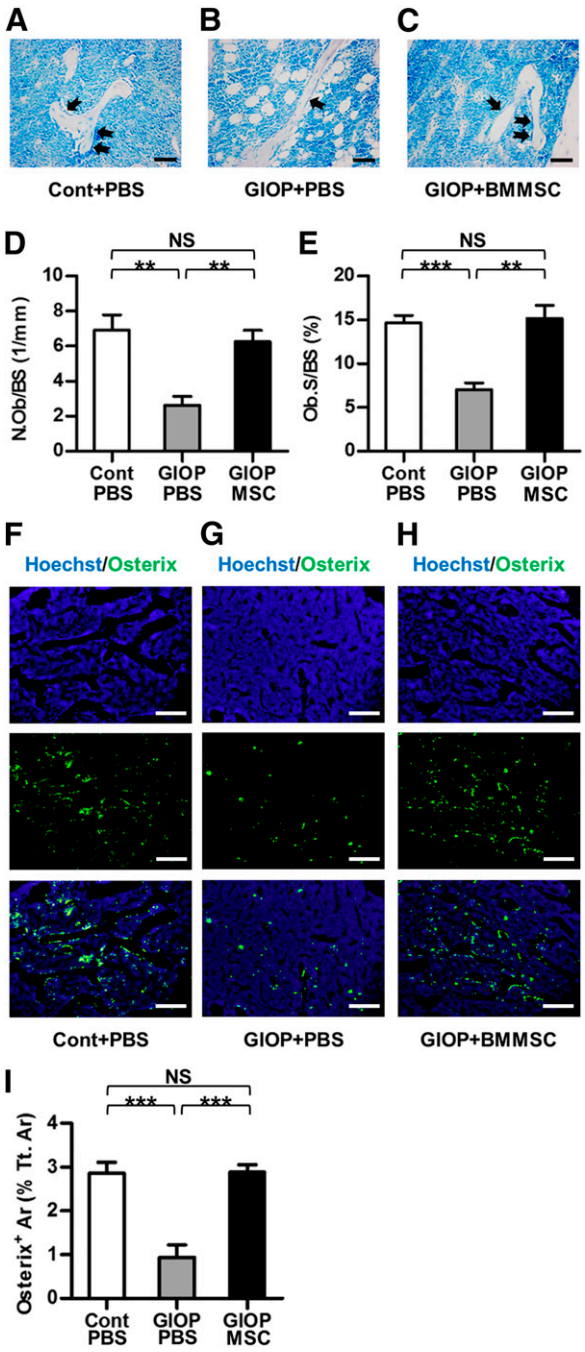

Figure 3. Survival of osteoblasts and osteoblast progenitors in recipient bone marrow. **(A–C):** Representative toluidine blue-staining images exhibiting osteoblasts (black arrows). Unstained empty spaces represent occupied area by adipocytes in the bone marrow. Scale bars: 50 μm. **(D, E):** Corresponding parameters showing maintenance of osteoblast survival by MSC therapy. **(F–H):** Representative images demonstrating Hoechst staining for total cells (blue), Osterix immunofluorescence for osteoblast progenitors (green), and merged labeling. Scale bars: 200 μm. **(I):** Corresponding parameter showing maintenance of osteoblast progenitor survival by MSC therapy. Data represent mean $\pm$ SEM; n = 4 per group. **, $p < .01$; ***, $p < .001$. Abbreviations: Ar, area; BMMSC, bone marrow-derived mesenchymal stem cell; Cont, control; GIOP, glucocorticoid-induced osteoporosis; MSC, mesenchymal stem cell; NS, not significant; N.Ob/BS, number of osteoblasts per bone surface; Ob.S/BS, osteoblast surface over bone surface; PBS, phosphate-buffered saline; Tt.Ar, total area.

markers of bone formation (P1NP) and bone resorption (CTX-1) exhibited consistent results that MSC therapy primarily rescued the reduction of bone formation but failed to prevent the transient elevation of bone resorption (supplemental online Fig. 3B–3E). Additional analyses on concentrations of serological TNF-α and IFN-γ revealed no systemic modulatory effects of infused BMMSCs on inflammation (supplemental online Fig. 3F, 3G).

MSC Therapy Promoted Osteoblast and Osteoblast Progenitor Survival of Glucocorticoid-Treated Mice

To investigate whether the effects of infused BMMSCs on bone formation were attributed to the changes of osteoblasts, toluidine blue staining was performed. As shown in Figure 3A–3C and the corresponding parameters (Fig. 3D, 3E), glucocorticoid treatment induced loss of osteoblasts and increase of adipocytes in bone marrow, which could be prevented by MSC therapy.

We next examined whether the promotion of osteoblast survival by MSC therapy was attributed to an increase in osteoblastogenesis. Immunofluorescence labeling analysis was performed to detect Osx$^+$ osteoblast progenitors in recipient bone marrow. As shown in Figure 3F and 3G, glucocorticoid treatment reduced the number of osteoblast progenitors. BMMSC infusion promoted osteoblast progenitor survival in bone marrow (Fig. 3H), as indicated by maintenance of Osx$^+$ area (Fig. 3I).

Donor BMMSCs^{GFP} Inhabited Recipient Bone Marrow

We next examined whether donor BMMSCs engrafted and inhabited bone marrow by using GFP-labeled BMMSCs derived from GFP$^{+/+}$ transgenic mice in Experiment 3 (Fig. 4A). As depicted in Figure 4B–4D, donor BMMSCs^{GFP} migrated and homed to recipient bone marrow within 24 hours postinfusion and engrafted for at least 4 weeks postinfusion. The percentage of GFP$^+$ area in total bone marrow area was $>$2% at 24 hours postinfusion and slightly decreased to approximately 1.5% at 4 weeks postinfusion. No GFP$^+$ cells were noted in the GIOP+PBS group (Fig. 4E). Additionally, BMMSCs^{GFP} rapidly diminished in peripheral blood within 24 hours postinfusion, and virtually no GFP$^+$ cells in PBMNCs could be detected at 72 hours postinfusion (Fig. 4F). These findings indicated local functional effects of donor BMMSCs^{GFP} to promote bone formation and osteoblastogenesis in recipient bone marrow.

Donor BMMSCs^{GFP} Prevented Recipient Bone Marrow Cell Apoptosis

To further uncover the cell fate of donor BMMSCs in recipient bone marrow, TUNEL-GFP double-labeling analysis was performed at 24 hours postinfusion. As shown in Figure 5, BMMSC^{GFP} infusion prevented recipient bone marrow cell apoptosis at the sacrifice of partial apoptosis themselves. The apoptotic percentage of donor BMMSCs^{GFP} was less than 30%, suggesting survival of most infused BMMSCs^{GFP} to further function. No GFP$^+$ cells were detected in the control group or GIOP+PBS group (Fig. 5E).

Donor BMMSCs^{GFP} Committed to Osteoblasts With Induction of Recipient Osteoblastogenesis

We next investigated whether the inhabited BMMSCs^{GFP} participated in bone formation by performing a GFP-Osx double-labeling analysis at 4 weeks postinfusion. As shown in Figure 6, approximately 40% of donor BMMSCs^{GFP} underwent osteogenic differentiation into Osx$^+$ osteoblast progenitors (Fig. 6A–6D). Furthermore, the

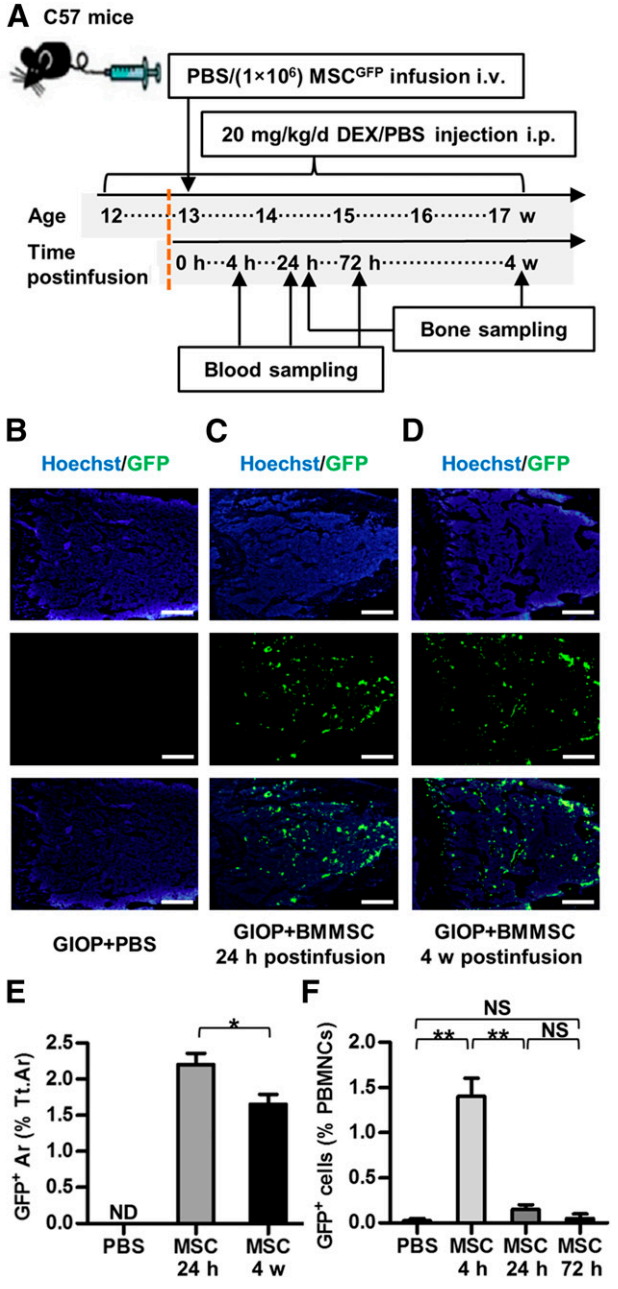

Figure 4. Study design of Experiment 3 and inhabitation of donor BMMSCs^{GFP} in recipient bone marrow. **(A):** Study design of Experiment 3 for cell fate investigation. Blood and bone were sampled at indicated time points. **(B–D):** Representative images demonstrating Hoechst staining for total cells (blue), GFP immunofluorescence for donor BMMSCs^{GFP} (green), and merged labeling. Scale bars: 500 μm. **(E):** Corresponding parameter showing inhabitation of donor BMMSCs^{GFP} in recipient bone marrow for at least 4 weeks. **(F):** Flow cytometric analysis of PBMNCs showing clearance of donor BMMSCs^{GFP} after 24 hours. Data represent mean ± SEM; $n = 4$ per group. *, $p < .05$; **, $p < .01$. Abbreviations: Ar, area; BMMSC, bone marrow-derived mesenchymal stem cell; Cont, control; d, day; DEX, dexamethasone; GIOP, glucocorticoid-induced osteoporosis; GFP, green fluorescent protein; h, hours; i.p., intraperitoneally; i.v., intravenously; MSC, mesenchymal stem cell; ND, not detected; NS, not significant; PBMNCs, peripheral blood mononuclear cells; PBS, phosphate-buffered saline; Tt.Ar, total area; w, weeks.

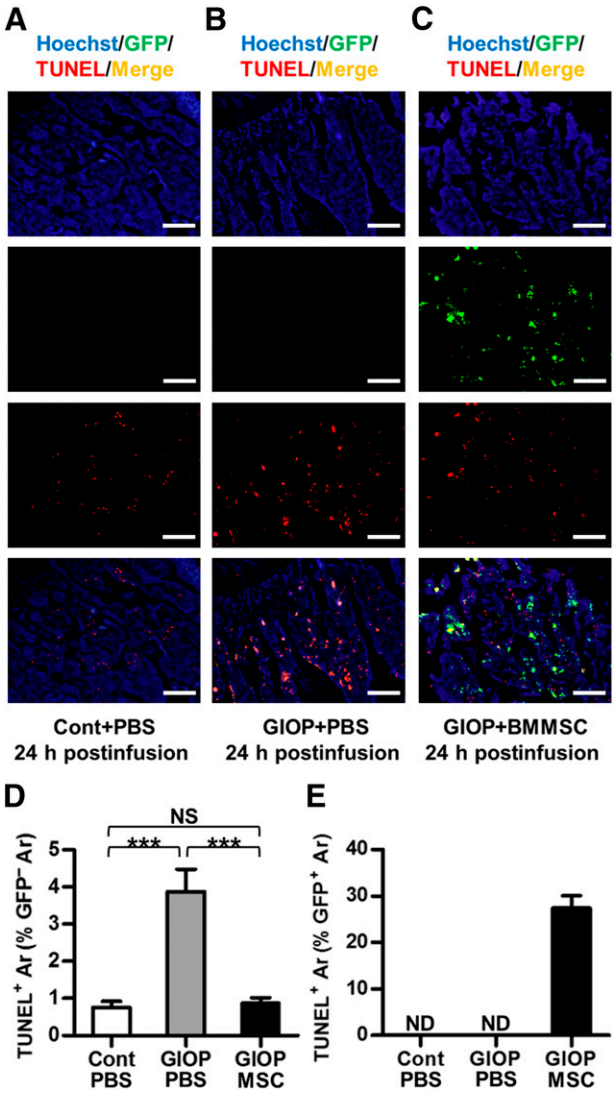

Figure 5. Donor BMMSC^{GFP} survival and apoptosis in recipient bone marrow. **(A–C):** Representative images demonstrating Hoechst staining for total cells (blue), GFP immunofluorescence for donor BMMSCs^{GFP} (green), TUNEL fluorescence for apoptosis (red), and merged double-labeling for apoptotic donor BMMSCs^{GFP} (yellow). Mice were sacrificed at 24 hours after PBS or BMMSC infusion. Scale bars: 200 μm. **(D, E):** Corresponding parameters showing partial apoptosis of donor BMMSCs^{GFP} with prevention of recipient bone marrow cell apoptosis. Data represent mean ± SEM; $n = 4$ per group. ***, $p < .001$. Abbreviations: Ar, area; BMMSC, bone marrow-derived mesenchymal stem cell; Cont, control; GIOP, glucocorticoid-induced osteoporosis; GFP, green fluorescent protein; MSC, mesenchymal stem cell; ND, not detected; NS, not significant; PBS, phosphate-buffered saline; TUNEL, terminal deoxynucleotidyl transferase-mediated dUTP nick-end labeling.

number of GFP$^-$Osx$^+$ osteoblast progenitors increased, suggesting induction of recipient osteoblastogenesis by infused BMMSCs (Fig. 6E).

Discussion

Excessive clinical use of glucocorticoids is a common cause of secondary osteoporosis [1–3]. In this preclinical study, we revealed that allogeneic MSC therapy could serve as a promising anabolic option in the management of GIOP, in that systemic infusion of BMMSCs

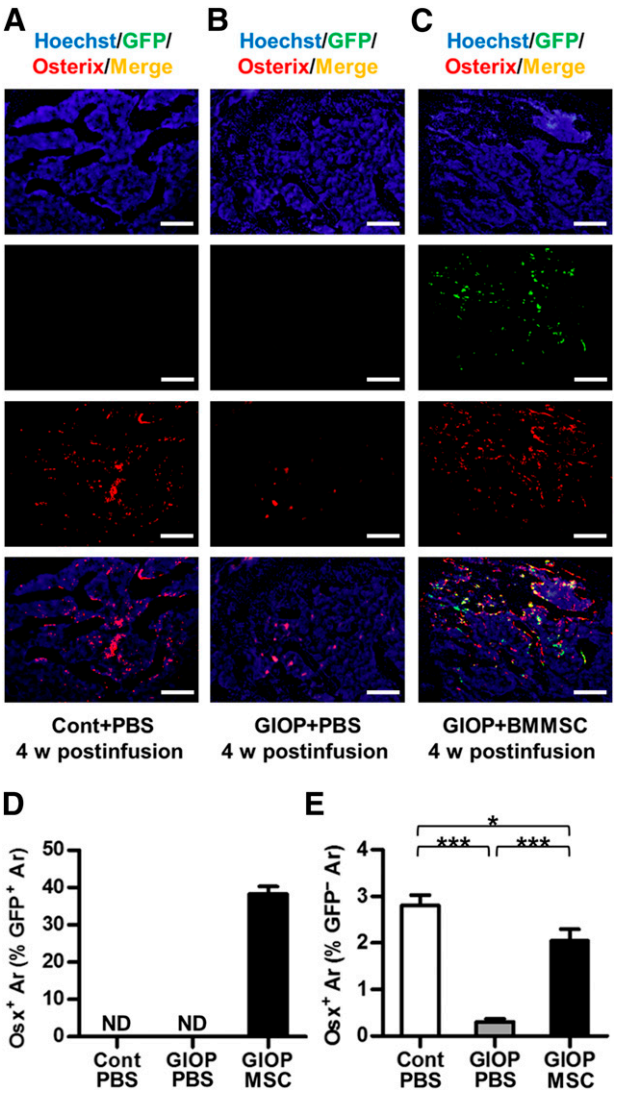

Figure 6. Osteogenic differentiation of donor BMMSCs^{GFP} and osteoblast progenitors in recipient bone marrow. **(A–C):** Representative images demonstrating Hoechst staining for total cells (blue), GFP immunofluorescence for donor BMMSCs^{GFP} (green), Osx immunofluorescence for osteoblast progenitors (red), and merged double-labeling for donor BMMSC^{GFP}-differentiated osteoblast progenitors (yellow). Scale bars: 200 μm. **(D, E):** Corresponding parameters showing osteogenic differentiation of donor BMMSCs^{GFP} with induction of recipient osteoblastogenesis. Data represent mean $\pm$ SEM; $n = 4$ per group. *, $p < .05$; ***, $p < .001$. Abbreviations: Ar, area; BMMSC, bone marrow-derived mesenchymal stem cell; Cont, control; GIOP, glucocorticoid-induced osteoporosis; GFP, green fluorescent protein; MSC, mesenchymal stem cell; ND, not detected; Osx, Osterix; PBS, phosphate-buffered saline; w, weeks.

prevented the reduction of both bone mass and bone strength in glucocorticoid-treated mice by maintaining bone formation. The MSCs we used were genetically unmodified, different from the CXCR4 and Cbfa-1 coexpressed C3H10T1/2 MSC-like cells adopted to treat GIOP in Lien et al. [5]. However, the allogeneic BMMSCs in our study exhibited potent cell homing efficacy with functionalized participation in recipient bone remodeling. As previously reported, being GFP$^+$ could have few effects on the performance of MSCs in implantation and retention [17], although we did not characterize GFP$^+$ BMMSCs ex vivo. It has been documented that freshly isolated MSCs display higher homing capability compared with their culture-expanded counterparts [27]. Our findings further suggested the feasibility of maintaining homing efficacy using allogeneic MSCs in clinical therapy of osteoporosis, without genetic manipulation.

The therapeutic potential of genetically unmodified allogeneic MSCs has been previously revealed in treating osteoporosis under inflammatory and autoimmune conditions in preclinical studies [8–10]. In murine models for postmenopausal osteoporosis and systemic lupus erythematosus-induced secondary osteoporosis, systemically infused allogeneic MSCs suppressed activated T cells via Fas ligand-mediated Fas pathway, which has been demonstrated as key to their therapeutic potential in preventing bone loss [8, 9]. However, one of the main differences between GIOP and postmenopausal osteoporosis is the distinct systemic environment, in that glucocorticoid therapy is widely used in autoimmune diseases to control inflammation [1]. Therefore, immunomodulation might not be included in the underlying mechanism of MSCs preventing GIOP, as shown in our study. In addition, the increase of bone resorption is also one of the common effects of excessive glucocorticoids that may be alleviated by MSC infusion [5, 9]. In this study, the bone resorption rate increased within 1 week of exposure to excessive glucocorticoids before dropping to the baseline level at 4 weeks, consistent with a report in humans [28]. Interestingly, BMMSC infusion did not prevent the transient increase of bone resorption, suggesting that the therapeutic effects were based on the maintenance of osteoblastogenesis.

There is growing evidence that infused MSCs have higher homing efficacies toward the bone marrow compartment or sites of inflammation and injury [13, 29], although a large percentage of transplanted MSCs could get sequestered in other tissues such as lung [5]. Previous preclinical research in osteoporosis revealed that through either enforced homing by CXCR4 or direct injection into bone marrow, transplanted MSCs could engraft and exert local anabolic effects [5–7]. However, the exact localization and functional characterization of inhabited MSCs remain exclusive. In our study, we first took advantage of GFP-labeled MSCs to investigate cell fates after homing. We found that most engrafted MSCs were retained, with less than one-third of them suffering apoptosis. We also revealed that of the surviving MSCs, approximately one-half participated as a functional part to replenish recipient osteoblast-lineage cells. Furthermore, MSC retention in bone marrow profoundly promoted recipient osteoblastogenesis and osteoblast survival. Further tests should be done to detect BMMSC^{GFP} retention in other tissue sites. According to the present data, the homed allogeneic MSCs functioned primarily through local trophic effects on recipient osteoblast lineage cells in GIOP. Thus, the interesting question that remains is how these cells supported the recipient osteoblast-lineage cells. Additional experiments are suggested to elucidate other types of cells that inhabited BMMSCs^{GFP} could differentiate into and to characterize the types of cells undergoing apoptosis, which might provide valuable information in the selection of cells for future use. Studies are also needed to uncover the molecular basis of donor-recipient interactions.

Conclusion

The therapeutic potential of genetically unmodified allogeneic MSCs in GIOP was revealed via systemic infusion. The therapeutic effects were based on maintenance of bone formation by donor MSCs inhabiting and functioning in recipient bone marrow, which in turn promoted osteoblastogenesis. These results provide important information regarding cell-based anabolic therapy for GIOP and uncover previously unrecognized MSC behaviors following a homing event.

Acknowledgments

This work was supported by grants from the National Natural Science Foundation of China (31301062, 81570937, and 81470710) and the National Basic Research Program (973 Program) of China (2011CB964700).

Author Contributions

B.S. and C.H.: conception and design, collection and assembly of data, data analysis and interpretation, manuscript writing, final approval of manuscript; X. Zhang, P.Z., T.H., C.Z., X.Q., and N.C.: collection and assembly of data, data analysis and interpretation, final approval of manuscript; X. Zhao, and Y.J.: conception and design, financial support, administrative support, provision of study materials, data analysis and interpretation, manuscript writing, final approval of manuscript.

Disclosure of Potential Conflicts of Interest

The authors indicated no potential conflicts of interest.

References

1 Rizzoli R, Biver E. Glucocorticoid-induced osteoporosis: Who to treat with what agent? Nat Rev Rheumatol 2015;11:98–109.

2 Henneicke H, Gasparini SJ, Brennan-Speranza TC et al. Glucocorticoids and bone: Local effects and systemic implications. Trends Endocrinol Metab 2014;25:197–211.

3 Mazziotti G, Angeli A, Bilezikian JP et al. Glucocorticoid-induced osteoporosis: An update. Trends Endocrinol Metab 2006;17:144–149.

4 Weinstein RS, Jilka RL, Parfitt AM et al. Inhibition of osteoblastogenesis and promotion of apoptosis of osteoblasts and osteocytes by glucocorticoids. Potential mechanisms of their deleterious effects on bone. J Clin Invest 1998;102:274–282.

5 Lien CY, Chih-Yuan Ho K, Lee OK et al. Restoration of bone mass and strength in glucocorticoid-treated mice by systemic transplantation of CXCR4 and cbfa-1 co-expressing mesenchymal stem cells. J Bone Miner Res 2009;24:837–848.

6 Cho SW, Sun HJ, Yang JY et al. Transplantation of mesenchymal stem cells overexpressing RANK-Fc or CXCR4 prevents bone loss in ovariectomized mice. Mol Ther 2009;17:1979–1987.

7 Zhang XS, Linkhart TA, Chen ST et al. Local ex vivo gene therapy with bone marrow stromal cells expressing human BMP4 promotes endosteal bone formation in mice. J Gene Med 2004;6:4–15.

8 Liu S, Liu D, Chen C et al. MSC transplantation improves osteopenia via epigenetic regulation of notch signaling in lupus. Cell Metab 2015;22:606–618.

9 Liu Y, Wang L, Liu S et al. Transplantation of SHED prevents bone loss in the early phase of ovariectomy-induced osteoporosis. J Dent Res 2014;93:1124–1132.

10 Ma L, Aijima R, Hoshino Y et al. Transplantation of mesenchymal stem cells ameliorates secondary osteoporosis through interleukin-17-impaired functions of recipient bone marrow mesenchymal stem cells in MRL/lpr mice. Stem Cell Res Ther 2015;6:104.

11 Lapidot T, Kollet O. The essential roles of the chemokine SDF-1 and its receptor CXCR4 in human stem cell homing and repopulation of transplanted immune-deficient NOD/SCID and NOD/SCID/B2m(null) mice. Leukemia 2002;16:1992–2003.

12 Komori T. Runx2, a multifunctional transcription factor in skeletal development. J Cell Biochem 2002;87:1–8.

13 Devine SM, Bartholomew AM, Mahmud N et al. Mesenchymal stem cells are capable of homing to the bone marrow of non-human primates following systemic infusion. Exp Hematol 2001;29:244–255.

14 Devine SM, Cobbs C, Jennings M et al. Mesenchymal stem cells distribute to a wide range of tissues following systemic infusion into nonhuman primates. Blood 2003;101:2999–3001.

15 Dempster DW, Compston JE, Drezner MK et al. Standardized nomenclature, symbols, and units for bone histomorphometry: A 2012 update of the report of the ASBMR Histomorphometry Nomenclature Committee. J Bone Miner Res 2013;28:2–17.

16 Liao L, Yang X, Su X et al. Redundant miR-3077-5p and miR-705 mediate the shift of mesenchymal stem cell lineage commitment to adipocyte in osteoporosis bone marrow. Cell Death Dis 2013;4:e600.

17 Ezquer F, Ezquer M, Contador D et al. The antidiabetic effect of mesenchymal stem cells is unrelated to their transdifferentiation potential but to their capability to restore Th1/Th2 balance and to modify the pancreatic microenvironment. Stem Cells 2012;30:1664–1674.

18 Stolzing A, Sellers D, Llewelyn O et al. Diabetes induced changes in rat mesenchymal stem cells. Cells Tissues Organs 2010;191:453–465.

19 Mei SH, McCarter SD, Deng Y et al. Prevention of LPS-induced acute lung injury in mice by mesenchymal stem cells overexpressing angiopoietin 1. PLoS Med 2007;4:e269.

20 Yang N, Wang G, Hu C et al. Tumor necrosis factor α suppresses the mesenchymal stem cell osteogenesis promoter miR-21 in estrogen deficiency-induced osteoporosis. J Bone Miner Res 2013;28:559–573.

21 Bouxsein ML, Boyd SK, Christiansen BA et al. Guidelines for assessment of bone microstructure in rodents using micro-computed tomography. J Bone Miner Res 2010;25:1468–1486.

22 Turner CH, Burr DB. Basic biomechanical measurements of bone: A tutorial. Bone 1993;14:595–608.

23 Wei J, Shi Y, Zheng L et al. miR-34s inhibit osteoblast proliferation and differentiation in the mouse by targeting SATB2. J Cell Biol 2012;197:509–521.

24 Zhang C, Tang W, Li Y et al. Osteoblast-specific transcription factor Osterix increases vitamin D receptor gene expression in osteoblasts. PLoS One 2011;6:e26504.

25 Oberhaus SM. TUNEL and immunofluorescence double-labeling assay for apoptotic cells with specific antigen(s). Methods Mol Biol 2003;218:85–96.

26 Gao LN, An Y, Lei M et al. The effect of the coumarin-like derivative osthole on the osteogenic properties of human periodontal ligament and jaw bone marrow mesenchymal stem cell sheets. Biomaterials 2013;34:9937–9951.

27 Rombouts WJ, Ploemacher RE. Primary murine MSC show highly efficient homing to the bone marrow but lose homing ability following culture. Leukemia 2003;17:160–170.

28 Dovio A, Perazzolo L, Osella G et al. Immediate fall of bone formation and transient increase of bone resorption in the course of high-dose, short-term glucocorticoid therapy in young patients with multiple sclerosis. J Clin Endocrinol Metab 2004;89:4923–4928.

29 Karp JM, Leng Teo GS. Mesenchymal stem cell homing: The devil is in the details. Cell Stem Cell 2009;4:206–216.

See www.StemCellsTM.com for supporting information available online.